Combined Raman spectroscopic and electrical characterization of the conductive channel in pentacene based OFETs

Beynor A. Paez S, Ilja Thurzo, Georgeta Salvan, Reinhard Scholz, Dietrich R. T. Zahn, and H. von Seggern[1]
Institut für Physik, Technische Universität Chemnitz, D-09107 Germany
[1]Fachbereich Material- und Geowissenschaften,
[1]Technische Universität Darmstadt D-64287 Germany

ABSTRACT

During the deposition of Pentacene on a Si-SiO_2 gate structure with Au bottom contacts for source and drain, the film growth was monitored with simultaneous *in situ* macro Raman spectroscopy and drain current measurements of the OFET device. The deposition of the active layer was carried out under UHV conditions at a growth rate of 0.65 Å/min. The purpose of the *in situ* characterization was to determine the minimum nominal thickness of the Pentacene layer required for efficient charge transport through the OFET circuit. At a thickness around 1.5 nm nominal coverage, the first percolation paths through the first organic monolayer develop, resulting in a sharp rise of the drain current. Up to a nominal film thickness of 30 nm, a subsequent slower increase of the drain current can be observed, revealing that the percolation of the first monolayer continues on a slower pace up to rather thick organic layers. These *in situ* measurements were complemented by *ex situ* isothermal deep level transient spectroscopy (charge QTS)

1. INTRODUCTION

Organic based electronics has become very attractive for technological applications. The delocalised carriers in the π molecular orbitals make them suitable for the charge transport. Devices based on organic materials are cheaper and easier to manufacture compared to their inorganic semiconductor based counterparts. Several applications of organic based electronic devices are found in systems like price tags, plastic electronics, transparent displays, non-volatile plastic memories with gate insulators based on polymer ferroelectric materials [1-6].
Several experimental and theoretical investigations have attempted to understand and improve the quality of the organic layer and its interfaces in order to improve the performance of the real devices [6-9]. In this work the investigation of charge transport and the conductive channel formation in organic field effect transistors is carried out. The experimental investigation is performed by *in situ* current-voltage (I-V) and Raman spectroscopy measurements. Monitoring the current as a function of the Pentacene coverage starting from sub-monolayer coverage gives valuable information about coverage where the onset of charge transport takes place. Raman spectroscopy helps to probe the molecular vibrations and thereby provides information about the normal mode frequencies of the molecule. and the vibrational spectrum is a characteristic fingerprint of the investigated system. Information concerning the charge states processes at interfaces, or structural order in organic materials; are well identified using this spectroscopic technique [10-14]. In order to identify the charge carrier interaction with traps, on the OFETs *ex situ* charge Deep Level Transient Spectroscopy (DLTS) measurements were performed. These results give valuable information about the influence of traps on the majority and minority charge carrier energetic distributions [15]. An anomalous behavior of the DLTS signal observed in Pentacene based OFETs is similar to results that have been reported for GaAs MESFET structures [16]. Also, transient current $I_d(t)$ measurements were performed to determine the condition for reaching the steady state of the charge transport in the conductive channel and to determine relaxation constants. These measurements revealed a non-steady state behavior of the I_d-V_d characteristics for short time scales, i.e. below 5 min. It means that there is a strong influence of the stress biases i.e. V_g and V_d, respectively, on the charge transport. A first attempt to simulate these transient effects was done considering a model based on two exponential contributions to the I_d-V_d characteristics. The mathematical formalism relies upon the basis of the fractional calculus [17]. Although in the present work we did not go further in the

Organic Field-Effect Transistors IV, edited by Zhenan Bao, David J. Gundlach, Proc. of SPIE Vol. 5940 (SPIE, Bellingham, WA, 2005) · 0277-786X/05/$15 · doi: 10.1117/12.617511

modification of the well known transport equations, we consider the fractional calculus as mathematical tool to model the multi-exponential behavior of the $I_d(t)$-V_d characteristics; in the way of considering any continuous function to be expressed as a linear combination of Debye exponential functions rather than a single stretched exponential [18].
Nonexponential relaxation has been observed in the persistent behavior of the photo induced I_d current after the photon source is switched off [19]. Moreover, persistent photoconductivity in inorganic semiconductors [20,21], metastable transport effects in Pentacene single crystals due to bias dependent generation and quenching of defects [22] were reported.

2. EXPERIMENTAL

The OFET devices were fabricated using heavily doped *n*-type silicon substrates (3–5 Ωcm resistivity) covered by a high quality thermally grown oxide with a thickness of about 285 nm acting as gate electrode and gate oxide, respectively. A thin chromium adhesive layer was deposited on the entire oxide surface before a 50 nm Au layer was deposited. The Au source and drain electrodes were photolithographically structured. They are configured as interdigitated fingers with a channel length of 5 □m and a channel width of 20 cm [23]. Pentacene (Aldrich GmbH) was thermally evaporated from a Knudsen cell kept at 155 ^{o}C at a base pressure of $3.7x10^{-9}$ mbar with a deposition rate of 0.6 Å/min onto the pre-structured substrates.

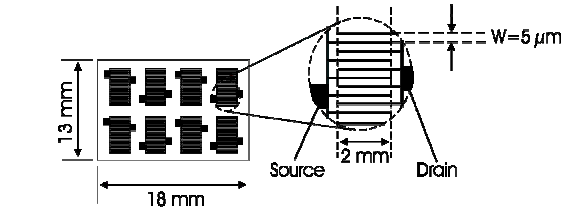

Length = 5 mm
Width = 20 cm
$dSiO_2$ = 285 nm

(a)

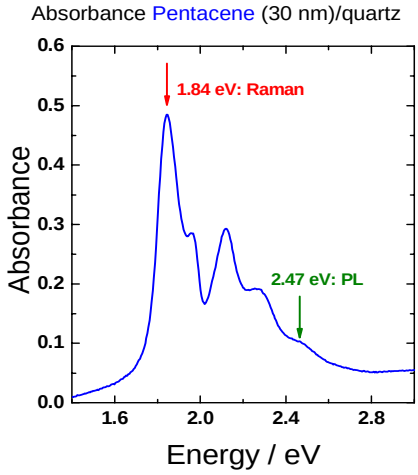

(b)

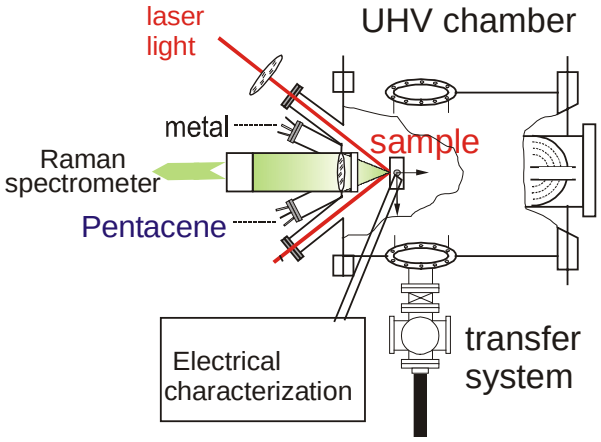

(c)

Figure 1. (a) Geometric sketch of the OFET structure layout, (b) absorption spectrum of Pentacene 30 nm / quartz, the arrows indicate the excitation energies maxima around which the Raman (1.916 eV) and photoluminescence (2.409 eV) measurements were done, respectively. (c) UHV system that allows to perform the *in situ* I-V characteristics and Raman measurements.

The *in situ* output characteristics of the OFET was measured with a Keithley 238 high current source measure unit. For the *in situ* Raman measurements the UHV system is optically aligned to a Raman spectrometer (Dilor XY) equipped with a CCD camera for multichannel detection in a quasi-backscattering configuration geometry. The sample was excited with the 647.1 nm (1.916 eV) Kr^+ laser line with a power density of (2825 ± 47) Wcm^{-2}. The excitation energy is close to the absorption maximum of Pentacene (1.84 eV) and thus allows resonant Raman measurements of the thin organic films to be carried out.
The *ex situ* isothermal deep level transient spectroscopy (charge QTS) were carried out with a charge-to-voltage converter (integrator) and processed by a three-channel correlator. Between the soured and drain contacts was applied a trap-filling pulse ranging between –1V and –10V. The measurements were performed with open gate contact.

3. RESULTS AND DISCUSSION

3.1. Simultaneous *in situ* I - V characterization and molecular vibration measurements of OFETs

Prior to the molecular evaporation the structure was electrically tested in order to check for possible leakage currents. Additionally, the Raman spectrum was taken to verify the absence of organic contaminants on the substrate before starting the pentacene deposition. During the step-wise molecular beam deposition the substrate was biased with a V_d = -10 V and Vg = -6 V. This allowed a continuous monitoring of the drain current in dependence on the organic film thickness.
The 3D plot shown in Fig. 2 shows the evolution of the Pentacene Raman bands with film thickness. On the right hand vertical scale the corresponding current value is plotted. Some intermediate Raman spectra are not shown for the presentation clearness.
From this *in situ* characterization it is clearly seen that for the earlier organic depositions, i.e. below 1.5 nm the Raman bands start to appear, while the drain current is approximately zero. This indicates the formation of molecular clusters which do not get form a conducting channel for the charge transport. At a nominal thickness of 1.5 nm the drain current increases abruptly and for further organic deposition there is an asymptotic increase of I_d. This result shows that the transport takes place in the layer in intimate contact with the gate dielectric. Although a low nominal coverage is enough to have charge transport in the OFET, it is not sufficient to protect the channel from deterioration when exposed to the atmospheric ambient, as observed in further experiments. At least a minimum amount of the organic or a capping material is required in order to have working devices under normal conditions.
The first monolayers behave as an organic boosting channel (OBC) where a high percentage of the nominal charge density is transported [24]. A similar effect has been observed on strained conductive channels in inorganic based transistors. For these devices a strained layer with typical thickness of 2.5 nm is used, as in the case of SiGe / s-Ge (2.5 nm) / insulator [24]. In Pentacene based OFETs the boosting channel is identified from the vibrational modes where there is a clear splitting of the band at 1157 cm^{-1} for high organic coverages (above 5 nm). This is an indication that for thinner organic layers the molecular/isolator interface is dominant. Raman measurements show that the 1st ML interacts with the substrate, or the molecular symmetry is lowered in the first layer.

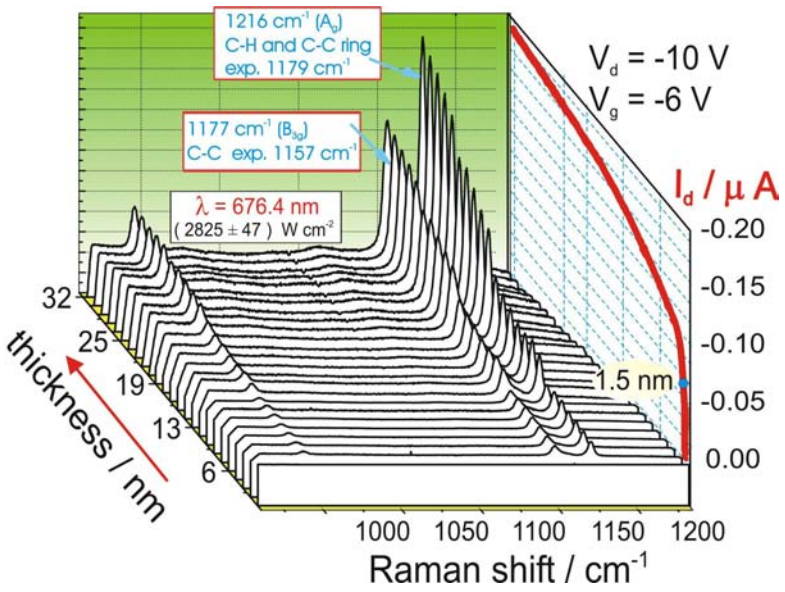

Figure 2. Simultaneous monitoring of Raman bands (black spectra) and drain current (red spectrum on the right hand side vertical axis) during the Pentacene deposition. The vibrational bands correspond to the in-plane molecular vibrations of Pentacene.

3.2. Vibrational bands profiling of the active layer

In situ measurements of the Raman bands were performed to identify the effect of different organic/inorganic interface formation in the channel. Fig. (3) shows the Raman intensity profile of Pentacene on the gold contact ranging from 0 μm to 900 μm, and on SiO_2 from 900 μm to 1100 μm. The circles in the figure correspond to the intensity of the C-H outer ring molecular in plane vibration at 1179 cm^{-1}. To highlight the metal / SiO_2 boundary position, the derivative of the signal was taken, leading to an asymmetric Gaussian like profile, localizing much better the metal/insulator interface. From this profile the semi half widths at full maximum (SFWHM) of the Raman signal from molecules on Au is found to be 41.1 μm, and for those on SiO_2 34.7 μm. Deconvoluting these SFWHMs with the laser line profile, one finds the effective SFWHMs for the Raman signal of Pentacene on Au and on SiO_2 of 14.6 μm and 8.2 μm, respectively. The found quantities indicate the effect of the boundary electrode upon molecules deposited on Au and those on SiO_2. Another effect that exhibit the molecules on the metal contact is the enhancement of the in the Raman signal, promoted by the roughness of the metallic surface, the interaction metal/Organics leads to the Surface Ehnacemente Raman Spectroscopy (SERS) [14] effect.
The difference between the two SFWHMs indicates that the organic layer on the metal is more influenced by the Au contact boundary effects than the molecules on SiO_2. The discrepancy is also an indication that the way of growing the organic layer in the vicinity of the metal / gate insulator interface is not uniform. A further possible hint for this effect is given by the steady state measurements of the electrostatic source-drain potential landscape. The potentiometry measurements performed with a Kelvin probe microscope have shown a non linear dependence of the potential through the channel (see Scholz *et al.*, in this proceedings), arising from a non-constant channel electric field parallel to the gated region and to a charge carrier density distribution through the active layer.

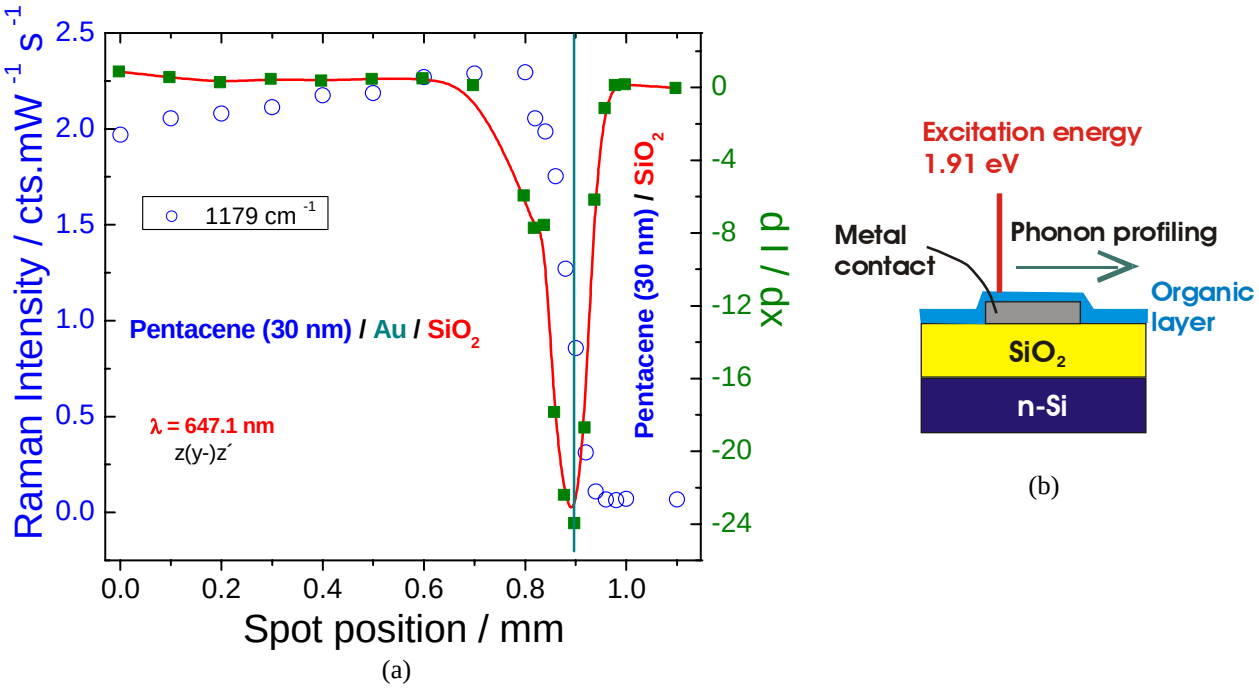

Figure 3. (a) Intensity profile of the Raman in Pentacene based OFETs, and (b) geometric sketch of the Au electrode of the pre-OFET structures used for the Raman measurements.

3.3. Bias stress-effects and multi-exponential current relaxation

From the I_d-V_d characteristics taken in darkness and under illumination, a decrease of the I_d current in time is observed. (fig 4).

In the OFETs the main transport is carried out in the first monolayers. On this connection in ref [25] it has been shown that the active charge carrier density is inverse quadratic proportional to the distance to the insulator. In the previous section the asymmetric influence of the organic/inorganic interfaces on the vibrational spectrum of the organic layer was identified. This can probably also influence the landscape drain-source potential. Additionally, we have observed a non steady stated behavior of the I_d-V_d characteristics, leading to a time dependent charge density, Fig. 4. On this occasion, we have considered the drain current as a time dependent quantity in order to estimate the dominant time scales to reach the steady state charge carrier density, mobility, conductance, transconductance. Due to the tendency of the numerous excitation-initiated natural phenomena to relax *via* exponential decay, the I_d is considered to be a linear combination of single Debye exponential functions. Given a well behaved function in a certain interval (continuous and differentiable), in general it can be linearly decomposed to an exponential basis set [14].

Following the above formulated idea, from the $I_d(t)$-V_d characteristics shown in Fig. 4, two time constants scaling the dynamic behavior of the drain current were determined.

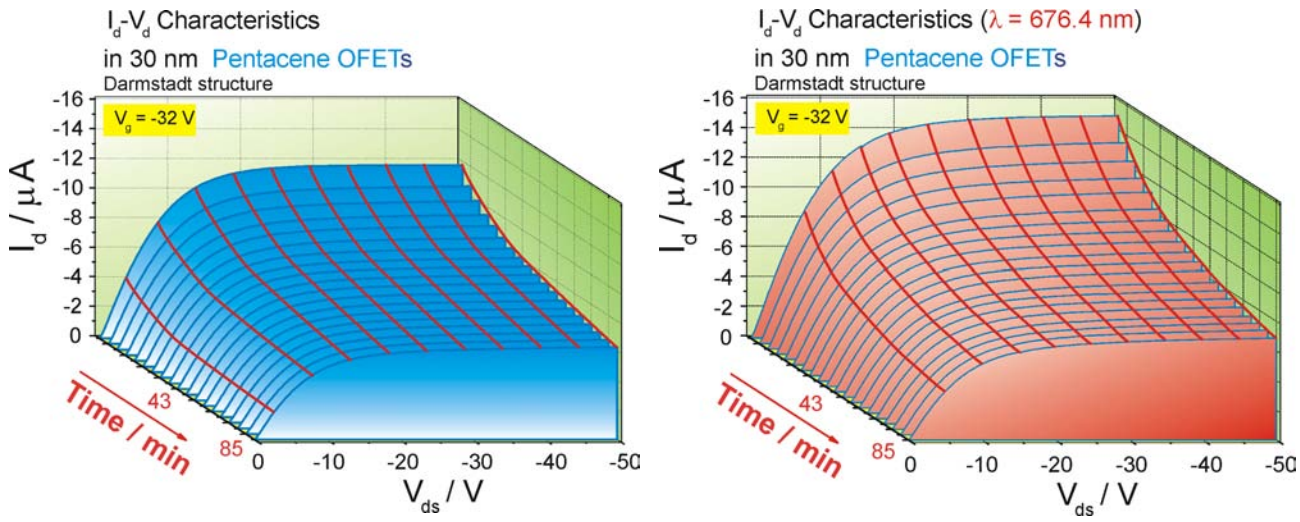

(a) (b)

Figure 4. Effect of stress bias on the I_d-V_d characteristics of OFETs (a) in darkness and (b) under illumination. The red contour lines indicate the time profile behavior of the I_d current for a fixed V_d voltage.

A first attempt to describe the I_d-V_d characteristics is given by

$$I_d = I_o + A_1 \exp(-t/\tau_1) + A_2 \exp(-t/\tau_2), \qquad (1)$$

being $I_o(t, V_d)$ the steady-state contribution to the current, A_1 and A_2 the coefficients weighting the exponential decay with time constants τ_1 and τ_2, respectively, the variable *t* is assumed to have a discrete value for each I_d-V_d characteristics with a drain bias scan rate of 10V/min.

The decomposition of an I-V curve using eq. (1) is shown in fig. 5. It must be noted that these coefficients depend on the bias voltages. Only remains the time dependence on the exponential functions which in this way can be intimately related to the physical properties of the organic layer i.e charge carrier interaction, charge density distribution, mobility. Further analysis are still under consideration by the authors.

The average estimated time constants in darkness and under illumination were quite similar $<\tau_1> = 59$ min and $<\tau_2> = 6$ min differing in less than 5%. The time constants determined from the I-V measurement taken in dark and under illumination indicates that for this excitation photon energy the trap density is preserved but not the charge carrier density. The electrical and vibronic experimental evidences suggest that a modified inorganic field effect transistor transport model must be considered..

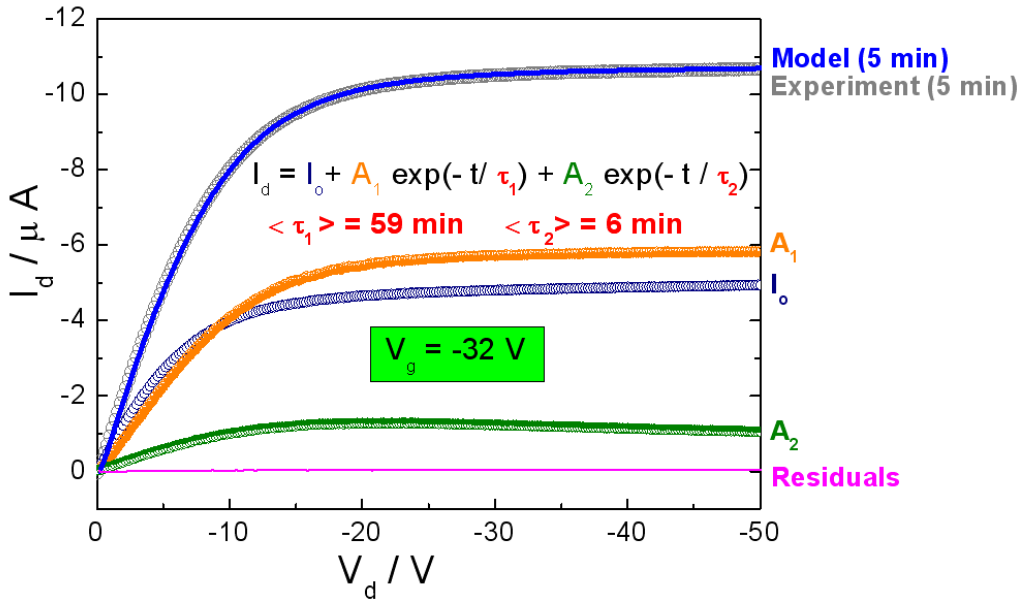

(a)

Figure 5. Simulation of one of the I_d-V_d characteristics shown in fig. 4. Experimental curves are plotted with circles. The quantities I_O, A_1, A_2, τ_1, τ_2,were determined from the red line-profiles shown in fig. 4. To reproduce here the experimental curve (top most curve), the time t is related to the drain sweep rate was, for this experiment 10 V/min.

3.4. Deep levels transient spectroscopy

The isothermal QTS measurements on a 30 nm Pentacene based OFET are sketched in fig. 6. The trap filling pulse U_1 is applied between drain and source with floating gate configuration. Then the charge carrier traps in the conducting channel under the gated region are recharged by this bias potential. The resulting exponential transient charge (after the pulse) is processed by a filter of time constants [15]

$$\Delta Q = Q(t_1) - 3/2\,Q(2t_1) + 1/2\,Q(4t_1). \qquad (2)$$

When scanning the delay t_1, the signal ΔQ is a maximum at $t_{1max} \cong \tau$.

Fig. 6(a) shows the DLTS signal for positive applied drain-source pulses which exhibits a linear dependence (Fig. 6(b)) between ΔQ and the pulse intensity. The trapping signal is coming from trapped holes, the majority charge carriers in Pentacene. Under special sampling conditions, it has been observed a reversed polarity of the ΔQ signal. Similar effects are also reported for GaAs MESFETs [16] with Schottky gate.

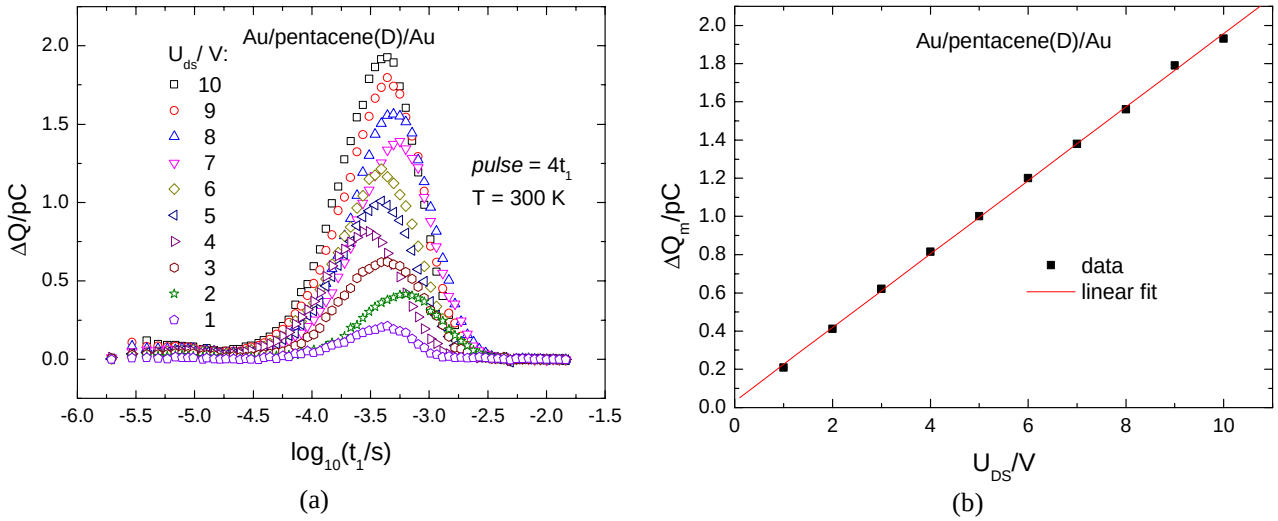

(a) (b)

Figure 6. Isothermal DLTS measurements in 30 nm Pentacene OFET, for filling traps a positive bias pulse U_1 is applied for 1 ms between drain and source. (b) Linear dependence of the mea.

CONCLUSIONS

Organic field effect transistors were characterized by *in situ* electrical and Raman spectroscopic measurements.

It was demonstrated that the first monolayers behave in a similar manner like a boosting channel in strained FETs. This result indicates that the charge transport in the channel is dominated by a 2D charge carrier gas. Although 1.5 nm Pentacene nominal coverage forms the conductive channel in the OFET, it is not enough to have stable devices performing under normal atmospheric conditions. Either a thicker coverage by the same organic material or a capping layer is required.

The Raman bands profiling indicate a strong effect of electrode edges upon the organic/inorganic interface formation, leading to a no uniform growth of the active layer. This effect is quite likely to promote non-constant channel electric field parallel to the gated region, and a charge carrier density distribution through the active layer. Additionally, time dependent $I_d(t)$-V_d characteristics showed that there are current relaxation effects that enrich the physics of the conductive channel i.e. charge carrier interaction, mobility, charge carrier distribution. On this concern, extended dynamic I_d-V_d measurements were carried out in two situations, in darkness and under illumination (1.916 eV). From both experiments similar sets of (two) time constants were determined, indicating that for this excitation photon energy the charge accumulation kinetics may be preserved, and the injected charge carrier density increasing under the illumination. The I_d-V_d characteristics were modeled considering a bias-dependent steady- state current combined with a linear superposition of two exponential current decays. With regard to the giant amount of the total transient charge (in mC range) either an accumulation of holes at the extracting (drain) electrode, or slow drift of the threshold voltage due to ion migration in SiO_2 should be taken into account as alternative mechanisms of the long-term instability.

The isothermal QTS measurements revealed a linear dependence between the positive drain-source pulse intensity and the ΔQ maximum coming from the majority trapped charge.

The Raman bands profiling and the electrical measurements evidence and suggest the necessity of an adequate transport model for organic field effect transistors.

ACKNOWLEDGEMENTS

This work was supported by the Deutsche Forschungsgemeinschaft (DFG) within the project Za 146/4-2 as part of *SPP 1121: Organic field effect transistors: Structural and dynamical properties.*

REFERENCES

[1] Research, European Semicond. **27 (4),** pp. 15 (2005)
[2] G. Horowitz, J. Mater. Res., **19**, 1946 (2004)
[3] H.-K. Kim, D.-G. Kim, K.-S. Lee, M.-S. Huh, S. H. Jeong, K. I. Kim, and Tae-Yeon Seong , Appl. Phys. Lett. **86**, 183503 (2005)
[4] S. Yoo, B. Domercq, and B. Kippelen, Appl. Phys. Lett., **85**, 5427-5429 (2004).
[5] Ch. J. Brabec, N. S. Sariciftci, and J. C. Hummelen, Adv. Funct. Mater. 2001, 15-26 (2001)
[6] C.N. Liab, C.Y. Kwonga, A.B. Djurisicc, P.T. Laia, P.C. Chuia, W.K. Chand, S.Y. Li, Thin Solid Films **477**, 57– 62 (2005)
[7] R. A. Street, J. E. Northrup, and A. Salleo, Phys. Rev. B 71, 165202 (2005)
[8] F. Schreiber, phys. stat. sol. (a) **201**, 1037 (2004)
[9] S. Scheinert, G. Paasch, I. Hörselmann, and A. Herasimovich, phys. stat. sol. (a) **202**, R82 (2005)
[10] G. Salvan, B.A. Paez¸ S. Silaghi, and D.R.T. Zahn, Microelectronic Engineering, ***in print***
[11] D. R. T. Zahn, phys. stat. sol. (a) **184**, pp. 41-50 (2001).
[12] P. Colomban, Spectroscopy Europe **15** (6), pp.8-16 (2003)
[13] D. Chenery and H. B. Smith, Spectroscopy Europe **15** (4), pp.8-14 (2003)
[14] B.A. Paez, G. Salvan, S. Silaghi, R. Scholz, T.U. Kampen and D.R.T. Zahn, Appl. Surf. Sci. **234**, 168 (2004).
[15] I. Thurzo, G. Pham, and D. R. T. Zahn, Semicond. Sci. Technol. **19**, 1075 (2004)
[16] J. H. Zhao**,** IEEE Transactions on Electron Devices, **37,** 1235 (1990)
[17] R. Hilfer, "Applications of fracional calculus in physcis", chap. 1, (World Scientific, Singapore, 2000)
[18] H. Schiessel and A. Blumen, J. Phys. A: Math. Gen. **26**, 5057-5069 (1993)
[19] S. Dutta, and. K.S. Narayan, Phys. Rev. B **68**, 125208 (2003)
[20] D. E. Theodorou, H. J. Queisser, and E. Bauser, Appl. Phys. Lett. **41**, 628 (1982)
[21] H. J. Queisser and D. E. Theodorou, Phys. Rev¸ B **33**, 4027 (1986)
[22] D. V. Lang, X. Chi, T. Siegrist, A. M. Sergent, and A. P. Ramirez, Phys. Rev. Lett. **93**, 076601 (2004)
[23] A. Hepp, H. Heil, W. Weise, M. Ahles, R. Schmechel, and H. von Seggern, PRL **91**, 157406 (2003).
[24] H. Shang, European Semicond. **27 (3)**, pp. 13 (2005)
[25] G. Horowitz, J. Mater. Res., **19**, 1946 (2004)